

U-BAD: ULTIMATE BURNED AREA DETECTION

Henrique Luis Godinho Cassol^{1,2}, Cesare di Girolamo Netto¹, Luciana Vanni Gatti², Luiz Eduardo Oliveira e Cruz de Aragão¹

¹ National Institute for Space Research (INPE), Remote Sensing Division ² Earth System Science Centre (CCST), Av. dos Astronautas, 1.758, São José dos Campos, 1227-010, São Paulo, Brazil; {henrique.cassol,cesare.neto,luciana.gatti, luiz.aragao}@inpe.br}

ABSTRACT

Here, we evaluated the combination of five satellites/sensors for improving burned area (BA) detection over the Amazon basin. Using a data set of 2,400 burn/no burn points by visual inspection in 2016, we investigated several spectral indices and ingested them into data mining algorithms to evaluate their burning area detection performance. Better results were provided with attribute selection combining Sentinel-2 (S2) and MODIS indexes (96 %), which were not significantly better than S2 indexes alone (95 %). The worst was the Sentinel-1 SAR data with 85 % accuracy. This is the first large-scale data research to evaluate the potentiality of combined temporal, spectral, and spatial resolutions for BA detection across the Amazon.

Index Terms — Rainforest, Carbon emission, Wildfires, Machine learning, Cloud computing.

1. INTRODUCTION

Drought severity and frequency are likely to occur in the future over Amazon, increasing the risk of forest degradation and carbon emissions due to biomass burning [1]. Besides the notable biodiversity reduction, there is a claim that it will also create positive feedback, culminating in the Amazon forest's new and unstable alternative state [2].

Therefore, it is imperative to provide accurate and annual fire scars in the Amazon with timely and low-cost detection. As in [3], the leading global products use the resources of one or two satellites/sensors to provide annual fire scars. Therefore, there is a trade-off between spatial resolution and temporal resolution. High spatial resolution sensors (~30 m) often detect small fire scars but lose many scars due to low revisiting time in cloudy environments, such as the Amazon. On the contrary, low spatial resolution sensors (~500 m) can detect many fire scars quickly but lose small ones. So, we evaluated five satellites/sensors in

combination to improve temporal and spatial resolutions to detect fire scars in the Amazon basin.

First, we identify 2,400 burn/no burned points across the Amazon basin in 2016 by visual inspection through time series of the set of sensors in a cloud processing Google Earth Engine (GEE). Second, several spectral indices commonly reported in the literature were ingested in a data mining algorithm to perform classification. The accuracy of classification was provided by overall accuracy, root mean square error and current burning maps comparisons.

2. MATERIAL AND METHODS

The study area encompasses the Amazon basin, including boundaries to the Cerrado biome, according to Eva et al. [4].

2.1. Sampling collection

We collect 2,400 burn/no burn point by visual inspection across the Amazon basin (Fig. 1), using time series analysis, active fire data (FIRMS), and burned area (MCD64) to train the algorithm.

We used time series to identify pixels that have an evident change in the vegetation index time series (e.g. NBR, normalized burned ratio) coincident with the burn date from MCD64 (see example in Fig. 2) and labelled to the burned pixel. Thus, no burned pixels were identified by pixels with no changes in the time series.

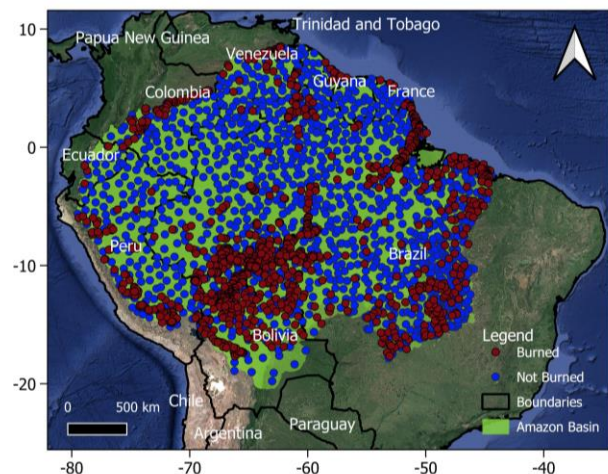


Figure 1. Points of burn/not burned across Amazon Basin.

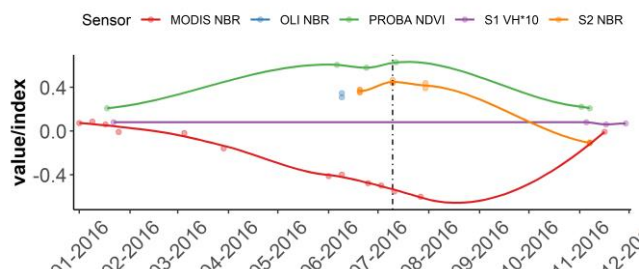


Figure 2. Time series of each sensor showing the burned date (vertical line) and the available images throughout the year (dots).

Almost 50% of the pixels were observed as burn between August to September (Fig. 3a) and with confidence >70% by FIRMS data (Fig. 3b).

2.2. Datasets

Five satellite/sensors were tested and had spectral indexes extracted to create a data set available on GEE: i) OLI Landsat 8 surface reflectance 30 m; ii) MODIS MOD09A1 V6 surface reflectance 8-day Global 500 m; iii) Sentinel-1 SAR GRD C-Band 10 m geocoded, iv) Sentinel 2 TOA reflectance 10-60 m, and v) Proba-V 100 m 3-day composites.

2.2.1. Preprocessing data

The multispectral data were first filtered using a cloud mask at each of the four multispectral sensors. Then, several spectral indexes often used to detect BAs (e.g. NBR, NDVI, NDMI) were calculated for each sensor when all bands were available. For instance, there is no SWIR-2 in PROBA-V. Besides, we processed the linear spectral mixture model to provide the soil, shade, and vegetation fractions at each multispectral sensor [5].

For S1, a median filter combined with a multitemporal QueganYu filter was applied [6]. Backscattering was previously transformed to linear scale and gamma values. The attributes were the two polarizations VV and VH, the ratio (VH/VV), the normalized difference (VV-VH/(VV+VH)), and the difference (VV-VH), mean ((VH+VV)/2), and sum (VV+VH) between them.

We performed temporal reductions in the annual time series GEE over Amazon mask at each band, such as percentile 0.9 and 0.1, minimum and maximum value, standard deviation, and median.

2.3. Data mining

Two data mining algorithms were applied to spectral indexes and bands to determine the best subset of each sensor's data and combined (545 attributes). We have tested the CFS filter and Wrapper, both with 10-fold cross-validation with 1000 iterations [7,8].

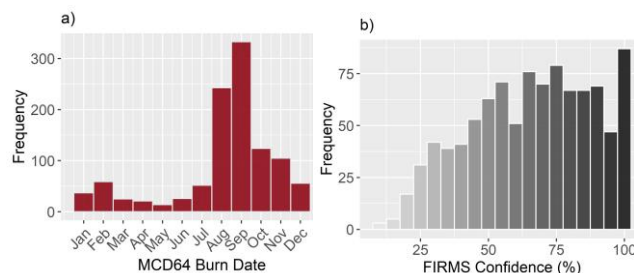


Figure 3. a) Frequency of burned points per month using burned date from MODIS. b) Confidence of active fire by FIRMS.

These techniques were applied to determine the best predictors to classify burn/no BAs in the Amazon with the least human intervention.

2.4 Classification

For classification purposes, we tested 10-fold cross-validation with the Random Forests algorithm, and the performance of each sensor and combined was provided with the following statistics: Overall accuracy (OA), Producer and User's Accuracy (PA & UA). Mean Absolute Error and Relative Mean Square Error (MAE and RMSE%).

2.4 Pos-classification

The classification result was masked, a posterior, by the Ground surface water product avoiding misclassification with inland water [9]. Also, a 3x3 kernel-mode filter was applied to reduce isolated pixels. Final classification was then exported in 100 m spatial resolution.

3. RESULTS

3.1. Spectral indices for burning detection

Data mining algorithms selected several spectral indices at each sensor (Table 1) and combined (Table 2). We highlight the Char-scar Index (CSI) (ρ_{NIR}/ρ_{SWIR2}), which the minimum value during the year indicates a high probability of such pixel being burned and appears as one of the best indices of the four optical sensors [10]. Other indices commonly reported in the literature as Normalized Burned Ratio (NBR) ($(\rho_{NIR} - \rho_{SWIR2}) / (\rho_{NIR} + \rho_{SWIR2})$) and (NBR2) ($(\rho_{SWIR2} - \rho_{SWIR1}) / (\rho_{SWIR2} + \rho_{SWIR1})$) were also a good indicator of burning [11].

The maximum and standard deviation of the Normalized Difference of Moisture Index NDMI ($(\rho_{SWIR1} - \rho_{NIR}) / (\rho_{SWIR1} + \rho_{NIR})$) and Mid-Infrared Burn index (MIRBI) ($(\rho_{SWIR2}) - 9.8(\rho_{SWIR1}) + 2$) have shown promising results in MODIS, OLI, S2, and Proba-V sensors [12, 13].

However, considering all sensors combined, CSI appears only in Sentinel-2, and no Sentinel-1 indices or bands were selected by any data mining algorithms (Table 1).

3.2. Overall performance after Wrapper selection

In general, the Wrapper algorithm performed well in selecting the best subset for classification purposes and was chosen to test classification accuracy.

Sensor	Best indices
Proba-V	CSI min, EVI min, NDCI p90, NDMI max, NDMI sd*, NDMI2 sd, NFDI min, Shade p10, Soil max, Soil p90, Veg min*, Veg p10
MODIS	B2 min, B3 min, CSI min*, MIRBI max*, MIRBI sd, NBR min*, NBR sd, NBR2 min, NBR2 sd*, NDMI max*, NDMI sd, NDVI sd, Shade min, Shade sd, Veg max
OLI	B1 p90, B5 p10, BAI max, CSI min, MIRBI max, MIRBI sd, NBR2 median, NBR2 min, NBR2 sd, NDWI sd
S2	B1 median, B2 max, B9 max, B9 median, B9 sd, B12 median, BAI sd, CSI min*, NBR min, NBR sd, NBR2 sd*, NDMI max, NDMI median, SAVI min, SAVI p10, Veg min
S1	(VV-VH) max, ((VH+VV)/2) p90, RGI median, RGI max, RGI sd, RPC2 median, VH median, VH min*, VV median, VV p90, VV sd
All	NDMI sd (Poba-V), EVI p90, MIRBI max*, MIRBI sd, NBR sd*, NBR2 min, NBR2 sd*, NDMI max (MODIS), B9 max, CSI min*, MIRBI sd, NBR min, NBR sd, NDMI max, SAVI 100 min, Veg min (S2), BAI p90, MIRBI sd, NBR2 sd, Veg min (OLI)

Table 1. Best indices for burned area detection. In asterisks the indices selected by both CFS and Wrapper algorithms.

Alone, each satellite/sensor's best subset has overall accuracy OA > 90%, excluding S-1 with OA = 0.82 (Table 2). In general, combined sensor's presented the lowest mean absolute error and RMSE (13.96 and 34.76%, respectively).

3.3. Burned area comparison

We computed a total BA for 2016 of 438,392 km² in red in Figure 4, representing roughly 5% of the whole Biome (7.2 Mi km²). This value corresponds threefold to the MCD64 product (143,610 km²). The most significant differences were observed in grassland in Bolivia and Roraima state in the Brazilian Amazon (Figure 5).

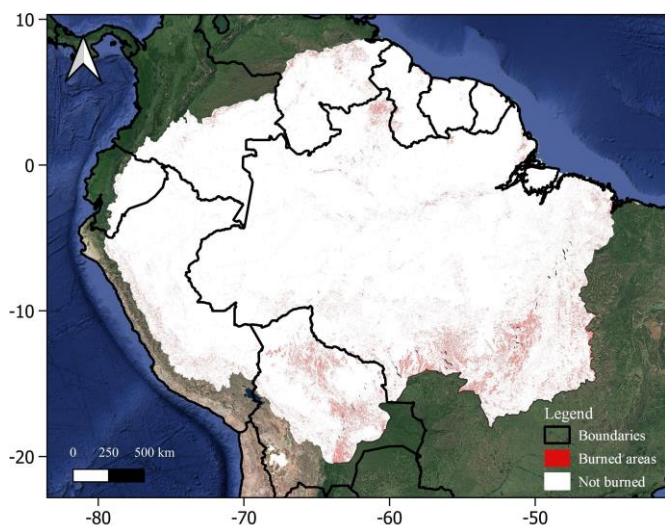


Figure 4. Classification using four multispectral sensors.

Sensor	OA	PA	UA	MAE	RMSE%
Proba-V	0.90	0.89	0.89	31.99	55.27
MODIS	0.92	0.90	0.94	24.38	48.48
OLI	0.90	0.89	0.91	28.54	52.19
S2	0.95	0.93	0.96	18.44	41.38
S1	0.82	0.85	0.80	52.27	72.22
All	0.96	0.96	0.97	13.96	34.74

Table 2. Overall accuracy and mean error of the classification after wrapper filtering.

4. DISCUSSION

4.1. Burned area detection

Burned areas detection in tropical regions is one of the major challenges in remote sensing for several reasons:

- i) Detecting surface or underground fires in dense forests can be detectable only by active fire sensors but untraceable for mapping using passive sensors. In addition, low-intensity and understory fires may not induce substantial changes in the canopy whereby optical sensors might detect, although this may impact forest functioning for several years [14,15,16].
- ii) Temporal difference between fire extinction and image acquisition. Post-fire vegetation can recover quickly in grasslands and open forests, which means that the gap for burned detection can be shorter than a singular satellite/sensor could provide, mainly in low-intensity fires. Also, understory fires are only identified based on multiple years of degradation patterns in spectral indexes [16]. On the other hand, more intense fires reduce the water content and produce more ash and charcoal that contrast with green vegetation reflection, which could be easily mapped. Therefore, the timing of burning is crucial for modelling forest fire emissions since biomass emissions factors and intensity vary seasonally [16].
- iii) Tropical regions are often covered by clouds, hindering BA detection, which requires active sensors and a synergic combination of multiple sensors to reduce the temporal resolution [3,17].

4.2. Estimation of burned area and techniques for classification

The total BA comprises almost three times what was provided by the MODIS 500 m product. Small burn scars mapped with Landsat 30 m resolution can increase up to 45% total BA over Cerrado compared to MODIS product [17]. Also, differences in the choice of the resolution of the product can represent 66% less fire carbon emission across Amazon using 30 m spatial resolution and 250 m [18]. Recent approaches combined Landsat imagery and a deep learning algorithm to improve BA detection, with an overall accuracy of 97% [19].

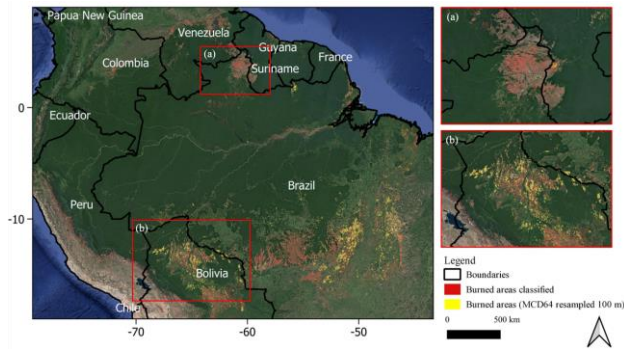


Figure 5. Comparison to MCD64 v6 product.

5. CONCLUSIONS

Machine learning techniques applied to ingest several remote sensing images on cloud computing can tackle one of the most challenging tasks: improving BAs' detection in tropical regions. Here, synergetic use of multiple satellite/sensors has detected three times more BA than using a single product (MCD46-MODIS). Also, the algorithm's performance was over 80% using a single satellite/sensor and at 96% when combined. The differences in BA detection have crucial importance for estimating burning emissions. Therefore, it is imperative having up to date algorithms to improve BA detection across Amazon.

ACKNOWLEDGEMENTS

The first author thanks FAPESP Grant #14423-4/2018.

8. REFERENCES

- [1] L. E. O. C. Aragão et al. 21st Century drought-related fires counteract the decline of Amazon deforestation carbon emissions,” *Nat. Commun.*, vol. (9), no. (1), pp. (536), Dec. 2018.
- [2] T. E. Lovejoy and C. Nobre. Amazon Tipping Point. *Sci. Adv.*, vol. (4), no. (2), p. (eaat2340), Feb. 2018.
- [3] L. Giglio, L. Boschetti, D. P. Roy, M. L. Humber, and C. O. Justice. The Collection 6 MODIS burned area mapping algorithm and product. *Remote Sens. Environ.*, vol. (217), pp. (72–85), Nov. 2018.
- [4] H. D. Eva et al., A proposal for defining the geographical boundaries of Amazonia; synthesis of the results from an expert consultation workshop organized by the European Commission in collaboration with the Amazon Cooperation Treaty Organization - JRC Ispra, 7-8 June 2005.
- [5] Y. E. Shimabukuro and J. A. Smith. The least-squares mixing models to generate fraction images derived from remote sensing multispectral data. *IEEE Trans. Geosci. Remote Sens.*, vol. (29), no. (1), pp. (16–20), 1991.
- [6] S. Quegan and Jiong Jiong Yu. Filtering of multichannel SAR images. *IEEE Trans. Geosci. Remote Sens.*, vol. (39), no. (11), pp. (2373–2379), 2001.
- [7] R. Kohavi and G. H. John. Wrappers for feature subset selection. *Artif. Intell.*, vol. (97), no. (1–2), pp. (273–324), Dec. 1997.
- [8] M. Hall. Correlation-based Feature Selection for Machine Learning. University of Waikato, 1999.
- [9] J.-F. Pekel, A. Cottam, N. Gorelick, and A. S. Belward, “High-resolution mapping of global surface water and its long-term changes,” *Nature*, vol. 540, no. 7633, pp. 418–422, Dec. 2016.
- [10] A. M. S. Smith, L. B. Lentile, A. T. Hudak, and P. Morgan. Evaluation of linear spectral unmixing and ΔNBR for predicting post-fire recovery in a North American ponderosa pine forest. *Int. J. Remote Sens.*, vol. (28), no. (22), pp. (5159–5166), Nov. 2007.
- [11] N. Benson and C. H. Key. Landscape assessment: Ground measure of severity, the composite burn index; and remote sensing of severity, the normalized burn ratio. Los Alamos, CO, 2006.
- [12] B. Gao. NDWI—A normalized difference water index for remote sensing of vegetation liquid water from space. *Remote Sens. Environ.*, vol. (58), no. (3), pp. (257–266), Dec. 1996.
- [13] S. Trigg and S. Flasse. An evaluation of different bi-spectral spaces for discriminating burned shrub-savannah. *Int. J. Remote Sens.*, vol. (22), no. (13), pp. (2641–2647), Jan. 2001.
- [14] M. Longo et al. Impacts of Degradation on Water , Energy , and Carbon Cycling of the Amazon Tropical Forests. *J. Geophys. Res. Biogeosciences*, vol. (125), no. (8), pp. (1–27), Aug. 2020.
- [15] D. I. Rappaport, D. C. Morton, M. Longo, M. Keller, R. Dubayah, and M. N. Dos-Santos. Quantifying long-term changes in carbon stocks and forest structure from Amazon forest degradation. *Environ. Res. Lett.* vol. (13), no. (6), 2018.
- [16] M. L. Humber, L. Boschetti, L. Giglio, and C. O. Justice, Spatial and temporal intercomparison of four global burned area products. *Int. J. Digit. Earth.* vol. (12), no. (4), pp. (460–484), 2019.
- [17] R. Libonati, C. C. DaCamara, A. W. Setzer, F. Morelli, and A. E. Melchiori. An algorithm for burned area detection in the Brazilian Cerrado using 4 μm MODIS imagery. *Remote Sens.* vol. (7), no. (11), pp. (15782–15803), 2015.
- [18] A. Carolina et al. Intercomparison of Burned Area Products and Its Implication for Carbon Emission Estimations in the Amazon *Remote Sens.*, vol. (12), p. (3864), 2020.
- [19] V. L. S. Arruda, V. J. Piontekowski, A. Alencar, R. S. Pereira, and E. A. T. Matricardi, “An alternative approach for mapping burn scars using Landsat imagery, Google Earth Engine, and Deep Learning in the Brazilian Savanna,” *Remote Sens. Appl. Soc. Environ.* vol. (22), p. (100472), 2021.